Received 23 September 2014
Revised 21 January 2015
Accepted 8 March 2015

Corrosion of bare and embedded in concrete steel bar – impact on mechanical behavior

Alkiviadis Apostolopoulos and Theodore E. Matikas
Department of Materials Science and Engineering, University of Ioannina, Ioannina, Greece

Abstract

Purpose – The purpose of this paper is to study the effects of corrosion on bare and embedded in concrete steel bars and additionally to study the impact on their mechanical behavior.

Design/methodology/approach – The mechanical properties on bare and embedded specimens of dual phase steel bar B500c were measured after tensile tests, before and after corrosion.

Findings – The results show superficial severe localized pitting corrosion of embedded specimens in contrast to bare specimens. Also recorded a significant influence of corrosion on the mechanical behavior of the embedded steel specimens in contrast to the corresponding bare specimens. The mechanical behavior of dual phase steel bar B500c, due to chloride induced corrosion, seems to be significantly influenced by the existence of local interactions and the intense of external pit depths of different inclusions (MnS and the FeS, etc.) close to the outer surface.

Social implications – The corrosion of concrete reinforcing steel, is the most common reason of "premature" degradation of structures in environments with chlorides. This creates justified concern in societies which exist in areas with particularly high seismicity such as the wider Mediterranean region. A large part of the structures in these countries are exposed to marine exposure conditions.

Originality/value – The originality in this paper is the research on bare and embedded specimens and the comparison between them and additionally are presented SEM and EDX analysis with interesting findings.

Keywords Mechanical properties, Chloride induced corrosion, Corrosion of steel bar, Pit depth, Pit depth and mass loss, Pitting corrosion

Paper type Research paper

Introduction

The corrosion of the rebars is a reason of "premature" degradation of structures in chlorided environment. This creates justified concern in societies in which there is a high level of seismicity such as the Mediterranean region. A large part of structures in these regions are highly exposed to marine conditions.

To this day, many casualties and enormous economic loss were resulted in earthquakes. After that, the scientific community paid closer attention to the seismic capability of building structures. One factor which can lead to catastrophic collapse, during an earthquake, is the fracture of the steel bar.

As a result, great importance was given to the systematic study of the mechanical upgrade of steel bar. To deal with such a challenge, before approximately 15 years, in the European Union was introduced one more economical production process which is known as "quenched and self-tempered" such as steel with high ductility B500c. This process achieved two things, first to reduce the production cost and second to increase the mechanical performance of steel bar by forming a hard exterior skin of self-tempered martensite. The strength of RC structures greatly depends on the bond between the rebars and the concrete. Many studies have revealed that corrosion existence reduces bonding between the rebars and the concrete.

International Journal of Structural Integrity
Vol. 7 No. 2, 2016
pp. 240-259

1757-9864
DOI 10.1108/IJSI-09-2014-0047

It is known that carbon steel bar embedded in concrete is passive to corrosive action by forming a thin layer of hydroxides due to the concrete alkalinity. In these cases, the presence of aggressive chloride ions destroys the passive film on reinforcing bar and as a result the corrosion rate becomes significant (Valcarce and Vazquez, 2009). At the same time the constant increasing emissions of CO_2 in the atmosphere reacts with the alkaline compounds of concrete which leads to pH decrease and consequent loss of passivity of the rebar (Ghods *et al.*, 2010; Ormellese *et al.*, 2006).

Porosity and cracks are the main factors that affect negatively the concrete quality, as their existence exacerbates the corrosion phenomena on rebars (ACI 318, 2011; Win *et al.*, 2004; MTO, SSP 904S13, 1995; Rostam, 2003).

However, these factors can be controlled by specific parameters associated with the composition of concrete and its maintenance (Ramezanianpour and Malhotra, 1995; Ballim, 1993; El-Sakhawy *et al.*, 1999).

Despite the fact that EN 1504 standard (BS EN 1504-5, 2013, British Standard) is valid in all European Union countries and provides all the necessary actions to restore and strength of structures, societies do not follow exactly the EN 1504 standard; first, due to lack of information and second due to the economical problems which exist.

Nowadays, non-destructive methods are applied for the monitoring and the evaluation of corrosive effects in RC structures. During the past decades, some non-destructive methods have been developed. Useful and very promising measurements are made with electrochemical methods such as: potential mapping, corrosion rate measurement, etc. Despite the fact that the non-destructive methods are used widely, they are still in stage of development.

Half-cell potential mapping is a simple and widely used technique for the on-site evaluation of corrosion risk in RC structures. ASTM C876-9 proposes a correlation between half-cell potential values and corrosive activity. However, several studies highlighted that various parameters can modify these absolute potential values without expressing a modification of the corrosion degree on steel surface (Ryell *et al.*, 1999; Francois and Arliguie, 1999).

For example, half-cell potential value can be affected by the chemistry of the water in the pores of concrete at the steel-concrete interface, regardless of any corrosion activity. These often lead to misinterpretation of half-cell potential measurements in RC structures (Poursaee and Hansson, 2008).

The non-destructive methods are unable to detect the localized damage of steel such as pit corrosion. Localized corrosion of steel bar is a very common situation in coastal areas and in many industrial regions. Chloride-containing solutions usually play a crucial role in pitting initiation. To this day, many attempts have been made to explain the pitting initiation of steel in chloride-containing solutions (Kolotyrkin and Popov, 1982; Strehblow, 1995; Apostolopoulos *et al.*, 2013).

Relatively limited work is identified with the corrosion effect of bare and embedded specimens and the issue of comparison between the mechanical properties and the investigation of depth of pit corrosion. The study of Stewart and Al-Harthy (2008) presents an interesting research of pitting corrosion and structural reliability of RC structures with experimental data and probabilistic analysis. Similar results are presented in Apostolopoulos *et al.* (2013) study.

The detrimental effect of corrosion on the service life of RC structures has implied the development of various research projects on the description of electrochemical processes in reinforcing bars, simulation of corrosion conditions, mechanical consequences, monitoring tools, etc. (Andrade *et al.*, 2001; Moreno *et al.*, 2004; RILEM, 2003, 2004; Law *et al.*, 2004).

In general, studies with RC structures which are exposed to natural environment are limited, most of them are based on laboratory tests. These tests are essential for improving the understanding of the corrosion mechanisms on RC structures.

Recently it was demonstrated that steel bars which are subjected to laboratory salt spray corrosion tests may suffer from a loss of strength properties compared to mass loss, a relatively modest loss of strength but a significant loss of ductility (Apostolopoulos, 2009; Apostolopoulos and Papadakis, 2008; Cairns *et al.*, 2005; Du *et al.*, 2005a, b; Lee and Cho, 2009).

It is commonly accepted that corrosion of steel is directly linked to mass loss. Additionally, corrosion products iron oxides on steel, which occupy a larger volume than the lost material did. Consequence of the above is the spalling of coating of concrete, the drop of resistance properties and yield stress (R_p), drop of maximum strength (R_m) and dramatic drop in ductility properties such as the limit of uniform elongation (A_g) and energy density (U).

Experimental study (Papadopoulos *et al.*, 2011) presents a correlation factor between the natural corrosion and accelerated salt spray corrosion based on mass loss, mechanical properties of rebars and the corrosion exposure time. This correlation is: one day in accelerated salt spray corrosion corresponds (on average) to 79 days in the natural corrosion.

In general, has not been found a correlation factor, like the above, between bare and embedded in concrete steel bars.

The experimental work (Apostolopoulos *et al.*, 2013) was carried out in reinforced concrete specimens and in bare specimens, with steel type B500c, in salt spray corrosion. The experimental corrosion effects in both bare and embedded in concrete specimens are presented so as to investigate the depth of pit corrosion. According to the results, the drop of mechanical properties of embedded specimens was greater than the corresponding of bare specimens for the same level of mass loss. This paper is the continuation of Apostolopoulos *et al.* (2013) study.

In this paper, several characteristics and parameters were measured and recorded, by tests, SEM and EDX, such as the size and range of crack in concrete, the half-cell potential values, pit depth of steel and the mechanical properties of steel, to both groups of bare and embedded specimens of dual phase steel tempcore B500c steel. The main aim of this laboratory program, of accelerated salt spray corrosion, is the observation of the degradation of embedded and bare steel specimens under corrosive action.

Experimental procedure

For the purpose of simulating the natural corrosion in coastal sites, 60 specimens (30 bare steel specimens and 30 steel specimens embedded in concrete) were exposed to the corrosive environment in a laboratory salt spray chamber for time periods of 10, 20, 30, 45, 60 and 90 days. A fog of salt spray testing environment was maintained, with eight daily wet/dry cycles in accordance to ASTM Standard B117 (2003). The type of steel specimens was B500c and their nominal diameter 10 mm. Steel bars were delivered from Greek industrial, in ribbed bars form. The solution of salt spray environment was 5 percent NaCl and its pH range 6.5-7.2. The temperature inside the salt spray chamber was maintained at 35°C (+1.1-1.7)°C.

Tensile tests were carried out at the whole number of specimens according to ISO/FDIS 15630-1 (2002). Each bar had been cut to the tensile testing length of 520 mm. The tensile tests were carried out on a servo-hydraulic MTS 250KN universal testing machine. In these tests were evaluated the yield stress R_p, tensile strength R_m,

elongation to tensile strength A_{gt} and energy density U. At eight specimens, which were embedded in concrete for corrosion exposure time of 90 days, were evaluated certain characteristics values such as, width of cracks, pH and chloride concentration in the concrete and also carried out measurements of half-cell values and a potential mapping was created.

The steel bars embedded in concrete were put in cylindrical plastic tubes (used as concrete molds), with an internal diameter of 30 mm and a total height of 520 mm. The concrete C16/20 class which was used, was prepared with CEM IV cement type (according to EN 197) and cement mix with a water/cement ratio (W/C) of 0.6. The concrete class C16/20 and coverage 10 mm were chosen for two reasons: first, to gain quickly the effects of corrosion on steel; and second, to simulate the majority of the building stock of Mediterranean countries that was used the same concrete class B225 (C16/20) for many years.

In this study the experimental effects of corrosion in both bare and embedded specimens are presented first, to investigate the mechanical behavior of steel corroded specimens (bare and embedded) and second to show the maximum depth of pit corrosion at various times.

In order to examine the influence of the salt spray corrosion and the surface thickness variation of the steel specimens were cut and prepared in cross-sections. In these cross-sections of concrete steel specimen took place monitoring of the interface between two materials with the aid of SEM and EDX. Martensitic layer appears to be higher in the location of the ribs and lower between them. The preparation included sectioning, resin immersion, grinding and polishing. Nital was used for the chemical etching. A cross-section of a 10 mm nominal diameter steel bar was prepared, where the high hardness martensite constituent is followed by a softer bainite layer and a ferrite-pearlite layer. Furthermore, corrosion products and the new situation in the outer surface of steel B500c tempcore were identified.

A day after their creation, specimens embedded in concrete, were removed from the plastic tubes and stored for 28 days. Then, specimens were placed in the laboratory salt spray exposure chamber for various times. Additionally to the embedded specimens in the salt spray chamber were placed bare steel specimens for various times. The effects of corrosion on the surface of a bare and embedded specimen after exposure to laboratory salt spray environment are shown in Plates 1 and 2.

Plate 1.
Corroded "bare" specimen after 60 exposure days, with mass loss 8.20 percent

Plate 2.
Corroded "embedded" specimen after 60 exposure days, with mass loss 2.80 percent

After the end of each exposure period, the surrounding concrete of steel specimen was crushed so as the corroded steel bar to be revealed. At the next step, the formed oxide layer was removed from the surface of bare and embedded specimens, according to the ASTM Standard G1 (2011) specification. Specimens were weighed again and prepared for measurements. Furthermore, corrosion products and the new situation in the outer surface of steel B500c tempcore were identified.

Digital image analysis and an optical microscope were used to evaluate the geometrical features of pits, such as size (depth, area and pit form). An image analysis software was used to estimate the pit area.

All mechanical tests were conducted at room temperature using an Instron servo-hydraulic testing system with a constant elongation rate of 2 mm/min. The tensile tests are intended to provide information on: first, the measurements of basic mechanical properties, strength and ductility, vs time of exposure, of embedded and bare specimens; and second, the comparative study between the two test groups in relation to the reported mass loss due to corrosion.

Results

Measurements on concrete

After the corrosive procedure of eight embedded specimens for 90 days, on the concrete surface were caused elongated cracks, the breadth and length of which were measured. For mapping the cracks on the concrete surface, were measured the width of cracks in five distinct regions (10 cm length each one, I, II, III, IV, V). In Table I, the maximum values of the range of surface cracks and the corresponding location along of each specimen separately are shown.

According to the second law of Fick, the diffusion rate (of chlorides), the absence of crack in concrete depends on the concrete class, the cement type, the water-cement ratio and the degree of preservation after concrete casting.

For each different combination of these parameters, there are different conditions and therefore different input rate of chlorides.

The cracks on the surface of concrete, allows the easy entry of external aggressive factors (Cl-, water, oxygen) and as a result, the validity of this law of diffusion in this case is deficient. In Seung Jun Kwon *et al.* (2009) study, based on analytical equations, is presented a modified diffusion coefficient in concrete as a function of the width of each surface crack.

Table I.
Cracks along the specimens on the concrete surface after 90 days to corrosion

Distance from the start point of the specimen Specimen code	0-10 (cm) I Crack width (mm)	10-20 (cm) II Crack width (mm)	20-30 (cm) III Crack width (mm)	30-40 (cm) IV Crack width (mm)	40-50 (cm) V Crack width (mm)	Mean value of crack (mm) Crack width (mm)
1e	0.25	0.10	0.10	0.20	0.20	0.17
2e	0.30	0.40	0.45	0.35	0.40	0.38
3e	0.10	0.15	0.20	0.35	0.25	0.21
4e	0.15	0.15	0.20	0.10	0.15	0.15
5e	0.25	0.15	0.50	0.40	0.35	0.33
6e	0.25	0.35	0.30	0.40	0.35	0.33
7e	0.30	0.40	0.50	0.45	0.15	0.36
8e	0.25	0.40	0.55	0.35	0.20	0.35

The concrete class and the content of cement which were selected to this study, lead to diffusion coefficient (in the non-cracked) about $Dm = 2.07$ (m^2/s)$\times 10^{-12}$ (Kwon *et al.*, 2009).

The diffusion coefficient of chloride in concrete ($D(w)$), when there is surface cracking, is calculated from the following mathematical expression:

$D(w) = f(w) \times D(m)$, Οπου: $D(w)$: diffusion coefficient in the presence of crack.
$f(w)$: coefficient of cracking, $f(w) = (31.61 \times w^2 + 4.73 \times w + 1)$,
w: width of crack $\geqslant 0.1$ mm.

Table II was made based on these equations and the values of Table I. Table II presents the estimated diffusion coefficient in each separate position.

From the measurement of chlorides in the whole number of reinforced concrete specimens, it was found a dramatic overrun of the maximum conventional limit of chlorides (1.2 kg/m^3) which is set by EN 206.

Table II presents many values of diffusion coefficient for cracked specimens. Some values are 14 time larger than there is at non-cracked specimens (Dm). As a result, when there are cracks, a faster rate of chloride diffusion is expected.

Half-cell potential

The half-cell potential measurements have been made at eight specimens, which were embedded in concrete for corrosion exposure time of 90 days. These specimens were corroded at fixed environmental conditions (eight wet/dry cycles per day, pH values between 6.5 and 7.2, temperature inside chamber at 35°C (+1.1-1.7)°C and solution 5 percent NaCl). Figure 1 shows the results of half-cell potential measurements along the specimen. Figure 2 shows the results of crack width measurements along the specimen for 90 days of corrosion. Figure 3 shows the correlation between half-cell potential measurements and the corresponding crack width of concrete.

Mass loss

The test program of artificial corrosion in salt spray, included six tests for different periods of exposure (10, 20, 30, 45, 60 and 90 days). Totally, 60 specimens were used (30 bare and 30 embedded specimens). After these tests, the specimens were cleaned in accordance to ASTM G1 and maintained in cooling, away from humidity. Specimens were weighed again and their final mass compared to the corresponding initial mass in

Distance from the start point of the specimen Specimen code	0-10 (cm) I $D(w)$ (m/s^2)	10-20 (cm) II $D(w)$ (m/s^2)	20-30 (cm) III $D(w)$ (m/s^2)	30-40 (cm) IV $D(w)$ (m/s^2)	40-50 (cm) V $D(w)$ (m/s^2)
1e	8.61E-12	3.70E-12	3.70E-12	6.65E-12	6.65E-12
2e	10.90E-12	16.46E-12	19.73E-12	13.51E-12	16.46E-12
3e	3.70E-12	5.01E-12	6.65E-12	13.51E-12	8.61E-12
4e	5.01E-12	5.01E-12	6.65E-12	3.70E-12	5.01E-12
5e	8.61E-12	5.01E-12	23.32E-12	16.46E-12	13.51E-12
6e	8.61E-12	13.51E-12	10.90E-12	16.46E-12	13.51E-12
7e	10.90E-12	16.46E-12	23.32E-12	19.73E-12	5.01E-12
8e	8.61E-12	16.46E-12	27.25E-12	13.51E-12	6.65E-12

Table II. Calculation of the diffusion coefficient in cracked concrete

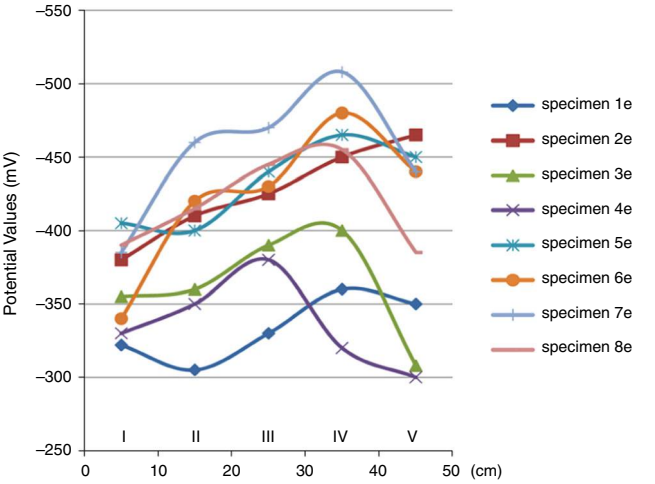

Figure 1.
Measurements of half-cell potential values along the concrete specimens after 90 days of corrosion

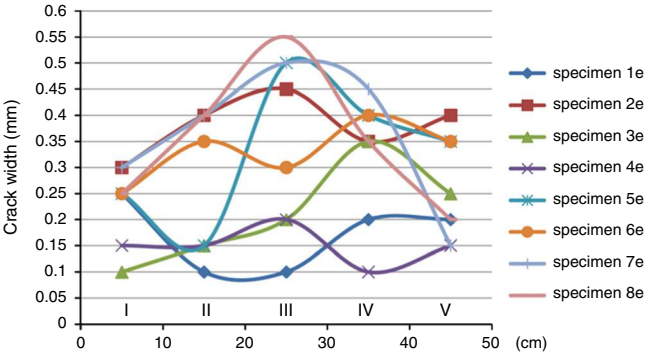

Figure 2.
Distribution of crack width along the embedded specimens after 90 days corrosion

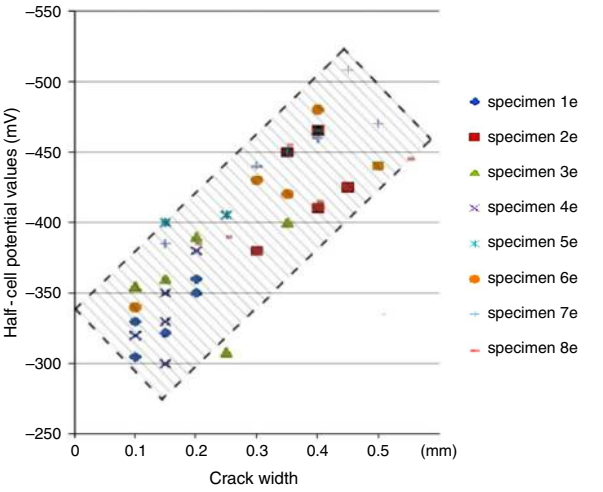

Figure 3.
Correlation between the distribution of half-cell potential values of corroded steel for mass loss 4.06 percent and crack width in concrete, after 90 days corrosion

order to evaluate the mass loss due to corrosion exposure. Table III shows the average values of mass loss of bare and embedded specimens. The mass loss percentage Δ_m is defined in the following equation:

$$\Delta_m = \frac{m_0 - m_c}{m_0} \times 100\% \quad (1)$$

where m_0 is the mass of non-corroded specimen and m_c is the reduced mass of the corroded specimen.

Measurements on steel bar

Pit examination

Examination of pits includes the next steps: Plate 3 and Figure 4, shows the bare and embedded specimens after cleaning (removing the products of corrosion and the concrete from the steel bar after accelerated corrosion tests). The area in green cycle is not yet corroded while in the red cycle spots there is localized corrosion and severe pitting. Plate 3 shows a typical view of corroded bare specimen. As it is shown between the two groups of steel bar, embedded specimens present more intense pits. Plate 4 presents a typical pit of an embedded specimen.

The first stage of the pitting process is related to the breakdown of the protecting passive oxide, the local conditions, the existence of specific factors such as thickness of oxides and also the chemical stability at the oxide-solution interface. The mechanisms which take place at the first stage of pitting have been proposed in Patrik Schmutz (2013) study.

Exposure time	Mass loss of bare (%)	Mass loss of embedded (%)
10 days	0.50	0.20
20 days	1.80	0.80
30 days	2.60	1.65
45 days	5.50	2.18
60 days	8.20	2.80
90 days	11.80	4.06

Table III.
The mean value of mass loss of bare and embedded specimens

Plate 3.
B500C Φ10

Note: Bare specimen with mass loss 8.20 percent

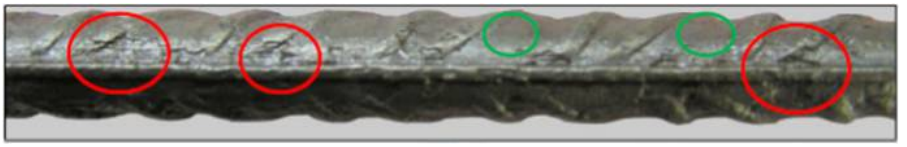

Figure 4.
B500C Φ10

Notes: Embedded specimen with mass loss 4.06 percent. Green cycle: non corroded area and red cycle: spots of localized corrosion that leads to severe pit corrosion

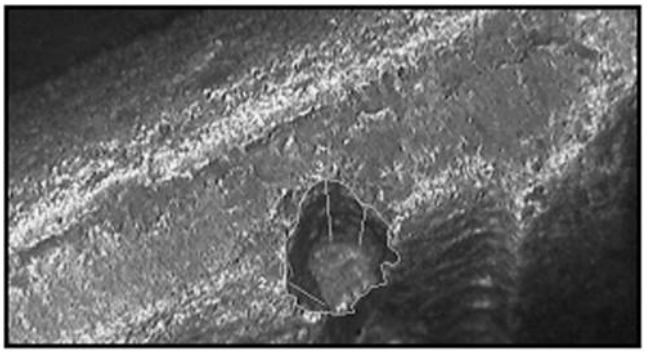

Plate 4.
A pit of an embedded specimen

The selected points of pitting show initially depths from 20 to 25 and 30 μm. Despite the difficulties of monitoring pits at their initial point, the conclusions lead to the opinion that generally many distinct possible scenarios of pit evolution occur. One way is by increasing the pit surface or maximum pit depth or with a combination of these two, with contemporary increase of the maximum pit depth and its surface as it is shown in Figure 5. In addition to these, a connection between neighboring pitting is observed. When two pits are closed, there is a possibility to be extended to a larger one. Pits are located to regions with high-stress concentration. These effects are evolving according to the local circumstances, the critical pit depth, the type of oxides which are produced and, etc. These conclusions are in agreement with Patrik Schmutz (2013), Nelson Silva (2013) and A. Turnbull *et al.* (2006) studies.

After monitoring and measuring the pit depth of specimens, we are able to express the view that the type of corrosion of bare specimens is similar to the Figure 5(b) and second to the Figure 5(a). In contrast, the type of corrosion of the embedded specimens is similar to Figure 5(c) and second to the Figure 5(a). From a macroscopic point of view, corrosion of bare specimens can be called uniform contrary to the type of corrosion of embedded specimens which is characterized with intense pitting.

As it can be seen in Figure 6, just from the early days of corrosion, pit depth of embedded specimens is significantly higher than the corresponding pit depth of bare specimens. In Figure 6 the maximum pit depths are presented. Values greater than 100 μm for embedded specimens and greater than 40 μm for bare specimens are chosen to be presented.

The values of maximum pit depth for each period of corrosion refer to five random specimens from each group (embedded and bare) for 20, 30, 45, 60 and 90 days of

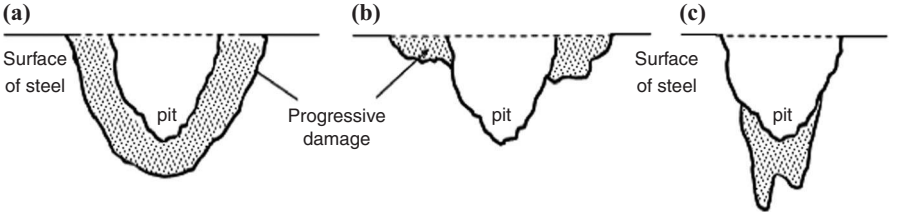

Figure 5.
Schematic illustration of a possible evolution of pits

Notes: (a) Increase of depth and surface of the pit; (b) increase of the surface of the pit; (c) increase of pit depth

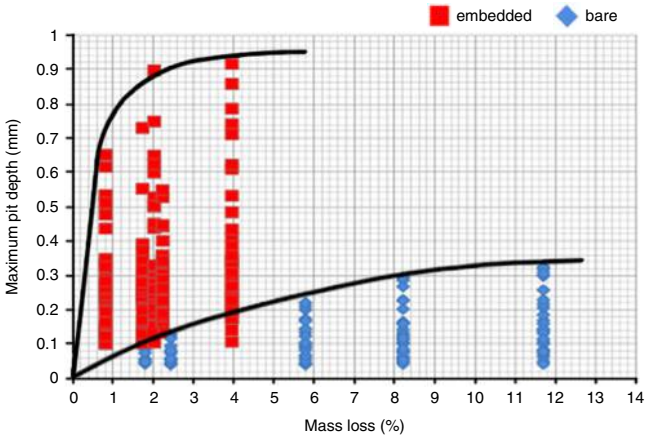

Figure 6.
Maximum pit depth on embedded and bare specimens and mass loss

corrosion. Each specimen was divided into five distinct regions (I, II, III, IV, V), 10 cm length each one. In Figure 6 the diagram of maximum pit depth vs mass loss is presented.

In Figure 7 the typical images from image J analysis of pits are presented. It is obvious that the most commonly occurring type of pitting on bare corroded specimens is a wide, shallow and elliptical shape. In embedded specimens dominates the vertical shape.

Mechanical properties of steel bar

Table IV presents the results of the mechanical properties of the two groups of specimens and the corresponding mass loss of steel B500c because of accelerated salt spray corrosion. Table IV shows the mechanical properties of yield stress and uniform elongation of B500c for bare specimens after 60 days time of exposure and for embedded specimens after 20 and 90 days time of exposure. The mechanical properties of yield stress and uniform elongation of B500c, are both extremely significant parameters in designing structures of reinforced concrete (as defined by Eurocode 2).

According to EC 2, steel type B500c is intended for structures which exist in seismogenic areas. B500c is characterized as steel with high ductility and strictly minimum values of acceptance for yield strength R_p(MPa). Additionally, it presents limit of 500 MPa and the same occurs for the limit of its uniform elongation A_{gt}(percent) to 7.50 percent and for the R_m/R_p rate which is between the following values, $1.15 < R_m/R_p < 1.35$.

Measurements of mechanical performance of non-corroded B500c steel bar, show a value of yield stress, $R_p = 529$ MPa and uniform elongation $A_{gt} = 12.80$ percent. Based on these properties, measurements of mechanical properties of specimens after certain periods of exposure to corrosive environment were conducted. The results analysis shows that the drop in ductility properties of embedded specimens corresponds to bare specimens with double mass loss. The dramatic drop of ductility properties can initially be explained by the values which are shown in Figure 6.

SEM, EDX

A research was conducted, with SEM and EDX, on specimens with section Φ10 of B500c steel, before and after various levels of salt spray corrosion. In both non-corroded and corroded specimens of B500c steel bar with high ductility, areas of MnS

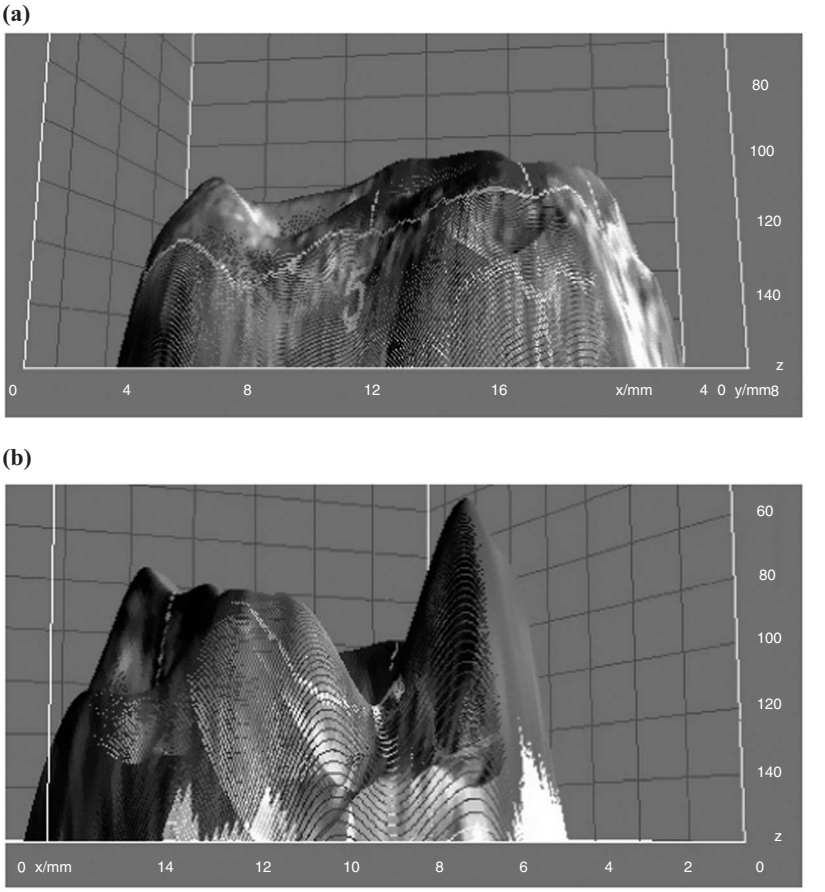

Figure 7.
Typical view of pitting on (a) bare and (b) embedded specimen

Specimen		Rp (MPa)	Agt (%)	Mass loss (%)	Specimen		Rp (MPa)	Agt (%)	Mass loss (%)	Specimen		Rp (MPa)	Agt (%)	Mass loss (%)
Bare (60 Days)	1b	503.5	7.80	7.35	Embedded (20 Days)	11e	521	11.45	0.81	Embedded (90 Days)	21e	508	7.05	3.50
	2b	500.6	8.10	8.95		12e	515	11.05	0.76		22e	492	8.38	4.90
	3b	484.4	7.95	9.20		13e	517	9.20	0.78		23e	515.5	7.60	3.65
	4b	482.3	8.10	8.40		14e	512	11.70	0.96		24e	505	7.40	4.30
	5b	471.5	7.60	7.10		15e	531	10.40	0.68		25e	502	7.30	3.95
Mean value		488.5	7.91	8.20	Mean value		519.2	10.76	0.80	Mean value		504.5	7.54	4.06

Table IV.
Results for mechanical properties of bare and embedded specimens for different exposure times of corrosion

Note: Numbers in red color are referred to drop under the minimum limits of EC 2

compounds were identified which, with the coexistence of other voids, constitute regions with degradation of consistency of steel material.

The MnS in non-corroded specimen was found with a maximum size of approximately 2 μm, in contrast to the corroded embedded specimens (60 days, mass loss = 2.80 percent) in which their size exceeded the value of 12 μm. The scattered MnS compounds and other impurities appear to be positioned at a distance between 10 and 3,500 μm from the surface and additionally more attention was given to MnS which is located in the hard martensite zone.

Plate 5 shows the SEM-EDX device and a cross-section of corroded specimen embedded in concrete, after 60 days exposed to chloride environment which was solidified with resin, for the elaboration procedure. Figure 8 shows the SEM images and elemental mapping (a) and (b) where the MnS compounds are distinguished by bright colors on the reinforcing steel surface after exposure to the corrosion, for mass loss 2.80 percent at pH = 6.5-7.5. In Figures high-density segregation of impurities which is close to the surface is distinguished. The impurities have been recognized via EDX to be Si and MnS (Si = dark color, MnS = gray color in EBSD). Figure 8(c)-(e) shows the existence of MnS (figures with red and yellow) at a distance of 350 μm from the external surface.

Figure 9 shows that the steel-concrete interface is occupied completely with corrosion products and this fully justifies the loss of connection between concrete and steel (bonding loss). Also it shows the degradation of cross-area of steel bar for 2.80 percent mass loss due to the exposure to chloride environment in which occurs strong damage due to the rapid deterioration of MnS areas with the risk of being joined with other surface pits (Rusteel Project, 2009-2012). This specific deterioration of MnS areas is adequately justified from the Webb *et al.* (2001) study in which is claimed 7that the pitting susceptibility of MnS inclusions in chloride-containing solutions is attributed to a preferential adsorption of chloride ions at these inclusions, which results in the chemical or electrochemical dissolution of MnS inclusions when the reinforcing steel is at a resting half-cell potential.

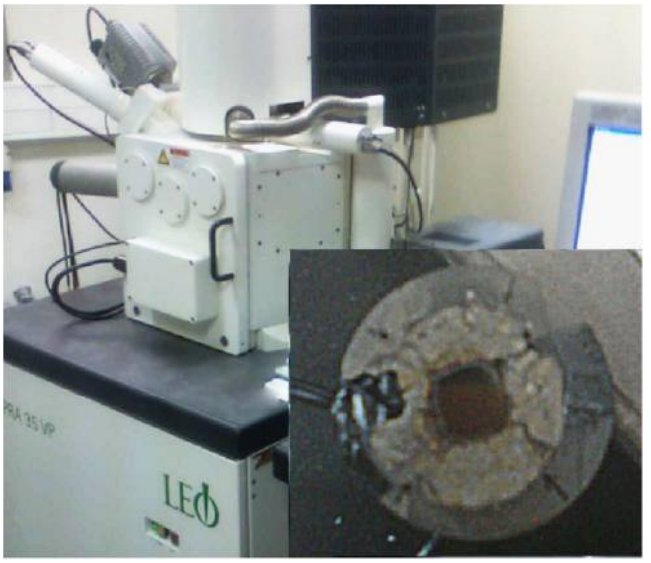

Plate 5.
A view of SEM-EDX device and a cross sectional of reinforcement corroded specimen B500c

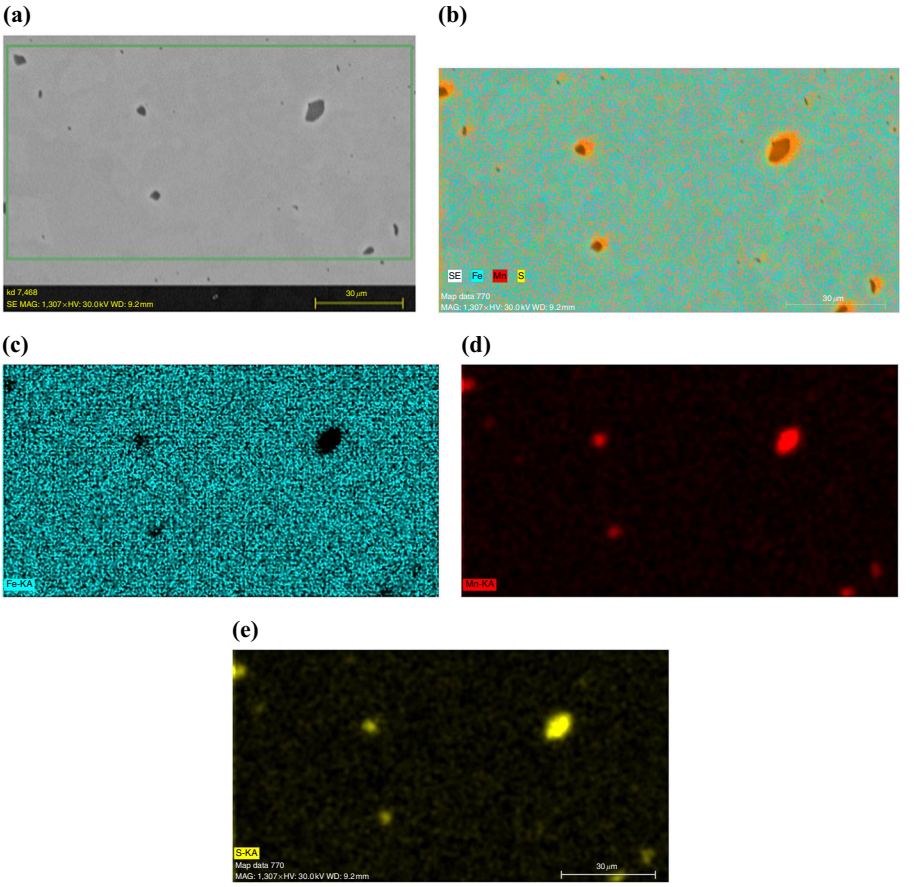

Figure 8.
High-density segregation of impurities close to the surface (350 μm) of corroded steel bar (2.80 percent mass loss)

Discussion

It is known that both oxygen and water when exist at the cathode, they contribute to propagation of chloride corrosion (Papadakis, 2000; Shi *et al.*, 2012). Despite the fact that in many studies chloride transport in concrete has been modeled using Fick's second law of diffusion, at many times there has not been taken into account the cracks interaction with the chloride diffusion.

It is also known that severe pitting corrosion exists even at low rates of O_2 (Ozbolt *et al.*, 2010). In this way it can take place severe corrosive effect without warning signs of corrosion stains on the outer surface of the concrete.

ACI 318 is a code of concrete structural design which takes seriously into account the existence cracks based on the fact that it is almost impossible to produce concrete without cracks.

Surface cracking due to corrosion of RC structures has been investigated by many researchers. Corrosion products press the reinforcing bar and this leads to the development of tensile stress in the concrete. In this way the cracking of surface begins. When corrosion is aggravated, cracks start to appear on the outer surface along the rebar and then the entry of aggressive factors (Cl-, oxygen and

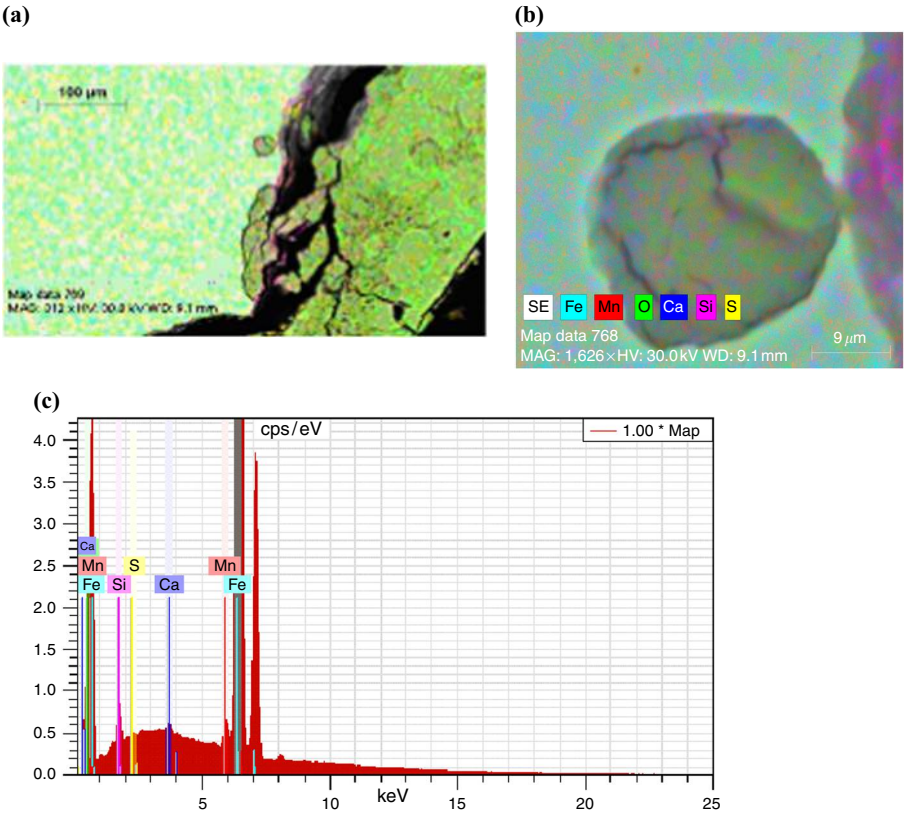

Figure 9.
Longer exposure (60 days) in chloride environment enhances phenomenon of close to surface or sub surface of (a) steel bar and (b) Fe oxides, Si oxides and (c)MnS

water) to the steel becomes easier, without the restrictions and the complex rules of law of diffusion.

After the above, the passive protection of the rebar has been lost, corrosion of reinforcing bar exists and this leads to rapid decline of the mechanical properties of steel bar (Cobo *et al.*, 2011; Apostolopoulos *et al.*, 2006; Apostolopoulos, 2007).

From Table II, it appears that the variability of crack width along the same specimen is an important reason that in the same specimen the diffusion coefficient varies from point to point up to six or seven times. The results show high levels of chloride diffusion in concrete specimens and this seems to be in relation to the high levels of half-potential values (Figures 1 and 2) or to point-intense mass loss of steel bar.

Observing the corroded specimens, there were two stages of cracking process. The first stage, of a few days period, with the initial cracks and the second stage, where most cracks grew gradually until they reached 0.55 mm.

Furthermore, it is important to mention that a reliable correlation between the degree of corrosion and the crack width is not possible. Measurements presented α scatter on these characteristics. This is probably due to non-uniform corrosion on the surface of rebar. Localized corrosion affects greatly to the extent of damage of corrosion and has shorter impact on the average crack width. Another possible reason may be that the increase of the width of the surface crack is affected by other cracks which occur inside the concrete.

Figures 1 and 2 show that the half-cell potential and width of crack values are in agreement to the small width of crack which corresponds to low values of half-cell potential. Figure 3 shows a linear correlation between half-cell potential values and width of surface cracks in concrete up to the value of 0.5 mm crack width. On the basis of these results, small widths of crack 0.1-0.15 mm on specimens correspond at half-cell potential values up to-400 mV which according to ASTM C876-9 denote that corrosive action exists. A prediction which can be expressed is that small widths of crack (0.1-0.2 mm) in structural elements of RC structures in salt spray environment can become critical for the useful life of the building and its structural integrity.

Mass loss

According to Table III, bare specimens, which were corroded in a salt spray chamber for a period of 90 days, present 11.80 percent mass loss. Embedded specimens present 4.06 percent mass loss for the same exposure period (90 days). Certainly, with higher concrete quality would be expected a lower mass loss of embedded specimens.

Pit

Pit measurements carried out along all the reinforcing bars from the early days of corrosion in order to research the pitting on surface of bare and embedded specimens.

Plate 3 and Figure 4 show that pitting corrosion is evident on both types of specimens. Corrosion attack begins at ribs of rebar and extend to the outer surface of rebar between the ribs.

After cleaning the specimens, maximum pit depth was measured stereoscopically. At the same time in order to compare the results, stereoscopic images were taken at the locations of the pits, (using a 35 mm magnification lens) converted to eight-bit gray-scale and normalized using special filter algorithms in order to bring the resolution and the lighting conditions to a common level according to the technique that was followed in C. Apostolopoulos *et al.* (2013) study. Figure 6 is based on results of 720 measurements.

Figure 6 shows that the embedded specimens generate greater pit depths. As it can be seen just from the early days of corrosion, pit depth of embedded specimens is significantly in a higher level than the corresponding of bare specimens.

In particular, from the initial days with mass loss 0.80 percent on embedded specimens the maximum pit depth reaches high values as 0.64 mm. On the contrary, on the bare specimens for over of three times higher mass loss (2.60 percent), maximum pit depth is only 0.135 mm. Bare specimens with 11.80 percent mass loss have 0.335 mm maximum pit depth. A testimonial of the aggression of corrosive action on embedded specimens are the pictures in Figure 7 where the main type of pitting is vertical type in contrast to bare specimens in which pitting has milder form. The influence of corrosive action of chloride ions on the steel bars depends on the source that they come from. In bare specimens chloride ions are derived solely from NaCl solution and in embedded specimens are first derived from $CaCl_2$ compounds (because of concrete) and after the extend of the cracks in the concrete are derived from NaCl. According to Jinxia Xu *et al.* (2011) study, the above version leads to pH changes. Bare specimens present higher levels of pH values compared to the embedded specimens. Additionally, embedded specimens have an increase in corrosion current density.

These results indicate that the corrosion process on the embedded steel bars is more severe than on bare rebars, probably due to a deeper and more extended pitting progress.

After the above, the general view can be expressed that in the embedded specimens is expected a higher concentration of mechanical stresses, for the same values of mass loss of bare specimens, due to the surrounding concrete cover. Indicative of the different corrosion damage in bare and embedded specimens are the Plate 3, Figures 4 and 7.

Similar conclusions about the adverse effects on embedded specimens as compared to bare specimens, incurred in C. Apostolopoulos *et al.* (2013) study.

In any case, it is interesting to examine the evolution of pitting with experiments for longer periods of corrosion exposure time.

Mechanical properties

Table IV shows that for 8.20 percent mass loss of bare specimens drop of the yield value was 7.65 percent (approximately equivalent to the mass loss) were calculated (as the ratio of the corresponding load capacity, divided by the initial, non-corroded, cross-section of the steel bars). The drop of the uniform elongation was 38.20 percent. In contrast, for 0.80 percent mass loss of the embedded specimens the drop of the yield value recorded (more than twice) 1.85 percent of the corresponding mass loss and also the value of uniform elongation measured close to 16 percent. In the group of embedded specimens for mass loss 4.06 percent, the drop of the yield limit measured in approximately 4.6 percent while the drop of the value of uniform elongation recorded at about 41 percent.

The most striking point of this analysis is the percentage reduction of uniform elongation as well as was increased significantly with time of exposure to salt spray chamber and is much higher than the corresponding percentage drop in yield strength and mass loss. The above results are relative to the results of C. Apostolopoulos *et al.* (2013) study.

The values of some specimens for R_p and A_{gt} were under or equivalent to the minimum that EC 2 requires ($R_p = 500$ MPa, $A_{gt} = 7.50$ percent). From the analysis of the results, indicates that the drop in ductility properties of embedded specimens corresponds to bare specimens with double mass loss. The different drop rate of ductility properties can initially be explained from the measured values of the maximum pit depth of the specimens (embedded-bare) as it is shown in Figure 6 and second due to the localized drop along the corroded specimens.

Similar issues of changes in cross-section diameter of rebars were investigated by other researchers in Cairns *et al.* (2005) and Du *et al.* (2005a, b) studies.

Program (DuraCrete, 2000) shows that a value of 0.3 mm crack width (from corrosive activity) is one of the criteria of service life of corroded RC structures. This value was observed at the same time for various beams which used in the program. Based on the findings of this research could be argued that: The surface crack width of 0.3 mm at low-strength concrete C16/20 as a criterion for end of service life of corroded RC structures just seems to be set for a new discussion.

MnS

According to R. Avci *et al.* (2013) study, during the manufacturing of carbon steel, in metallurgical processes, manganese is introduced into Fe (at a ratio of Mn to S of > 4) in order to scavenge the undesirable S impurities. Sulfur impurities are prone to forming FeS inclusions, which give rise to serious problems. The presence of MnS phases and FeS in steel rebar make the material highly susceptible to corrosion (and localized corrosion phenomena) due to the presence of chloride ions (Wranglen, 1969, 1974).

Figure 8 presents a high-density segregation of impurities close to the surface (distance 350 μm) of non-corroded steel bar many of which are MnS impurities. Figure 6 shows that on surface, immediately with the initial measurements of mass loss on embedded specimens, the depth of a large number of recorded pits is deeper than the regions that MnS inclusion exists (Figure 8).

Because of the fact that chlorides prefer to adsorb and accumulate at the MnS inclusions, it took place an increase of volume of MnS (Webb *et al.*, 2001). MnS areas play a leading role in the initial stages of internal corrosion of the steel bars. From Figures 8 and 9 and also from Apostolopoulos *et al.* (2013) and Rusteel Project (2009-2012) studies, it is obvious that critical side effects in terms of mechanical properties in sub-surface material dissolution create severe internal stress concentration.

The gradual volume increase of MnS compounds and FeS impurities which exist close to the external surface of steel bar, are accounted as areas without mechanical strength during the mechanical stress of rebars, however, develop severe internal stress concentrations creating conditions of interaction with other pits in the same position. After these, it is obvious that the different drop in ductility properties, between bare and embedded specimens, can be explained from the different pit depths. Attempting to evaluate the mechanical properties of embedded specimens as a function of the degree of reinforcement corrosion using the material constitutive laws of the study (Lee and Cho, 2009) failed to approach the results of mechanical properties (R_p and A_{gt}) of Table IV. One possible reason may be the coexistence inclusions and other external strong corrosion pits which measured and presented in present study.

Conclusions

In the current study are evaluated and presented the effects of the chloride induced corrosion on bare and embedded in concrete specimens of a dual phase Φ10 B500c steel bar, which were exposed to laboratory salt spray.

The specimens embedded in concrete present stronger superficial severe localized pitting corrosion in contrast to the bare specimens. That phenomenon was greater when the two groups of specimens were compared for the same mass loss. The corrosive action had a similar impact on the mechanical properties of the two groups of steel but for the same mass loss rate the embedded specimens presented greater drop of all mechanical properties.

The detection of areas on steel bar with MnS inclusions inside the martensitic zone and the fact that chloride prefers to be adsorbed and accumulate at the MnS inclusions constitute a serious reason of starting of internal corrosion of steel bar. The chloride induced corrosion presents a strong influence on mechanical performance of dual phase B500c steel bar because of the coexistence of external pits and the local interactions of various inclusions (MnS and the FeS) near the outer surface.

In conclusion, the dramatic decline in uniform elongation of embedded specimens can be justified by the followings.

First, that there was produced more severe pitting corrosion in terms of pit depth in embedded specimens compared to the bare specimens.

Second, to the combination of intense pitting with the rapid expansion of MnS areas with the simultaneous presence of chlorides. Also we must not ignore the specific characteristics of triple phase structure of B500c steel.

References

ACI 318 (2011), "Building code requirements for structural concrete", American Concrete Institute, Farmington Hills, MI.

Andrade, C., Keddam, M., Novoa, X.R., Perez, M.C., Rangel, C.M. and Takenouti, H. (2001), "Electrochemical behaviour of steel rebars in concrete: influence of environmental factors and cement chemistry", *Electrochimica Acta*, Vol. 46 Nos 24-25, pp. 3905-3912.

Apostolopoulos, A., Matikas, T., Apostolopoulos, C. and Diamantogiannis, G. (2013), "Pit corrosion examination of bare and embedded steel bar", *10th International Scientific and Technical Conference, Advanced Metal Materials and Technologies (AMMT'2013)*, *Saint Petresburg*, *June 25-29*, pp. 489-495.

Apostolopoulos, C., Demis, S. and Papadakis, V. (2013), "Chloride-induced corrosion of steel reinforcement – mechanical performance and pit depth analysis", *Journal Construction and Building Materials*, Vol. 38, January, pp. 139-146.

Apostolopoulos, C.A. (2007), "Mechanical behavior of corroded reinforcing steel bars S500s tempcore under low cycle fatigue", *Journal Construction and Building Materials*, Vol. 21 No. 7, pp. 1447-1456.

Apostolopoulos, C.A. (2009), "The influence of corrosion and cross-section diameter on the mechanical properties of B500c steel", *Journal of Materials Engineering and Performance*, Vol. 18 No. 2, pp. 190-195.

Apostolopoulos, C.A. and Papadakis, V.G. (2008), "Consequences of steel corrosion on the ductility properties of reinforcement bar", *Journal Construction and Building Materials*, Vol. 22 No. 12, pp. 2316-2324.

Apostolopoulos, C.A., Papadopoulos, M. and Pantelakis, S. (2006), "Tensile behaviour of corroded reinforcing steel bars BSt 500s", *Journal Construction and Building Materials*, Vol. 20 No. 9, pp. 782-789.

ASTM Standard B117 (2003), *Standard Practice for Operating Slat Spray (Fog) Apparatus*, ASTM Intern., West Conshohocken, PA. doi:10.1520/B0117-97.

ASTM Standard G1 (2011), *Standard Practice for Preparing, Cleaning, and Evaluating Corrosion Test Specimens*, ASTM International, West Conshohocken, PA.

Avci, R., Davis, B.H., Wolfenden, M.L., Beech, I.B., Lucas, K. and Paul, D. (2013), "Mechanism of MnS-mediated pit initiation and propagation in carbon steel in an anaerobic sulfidogenic media", *Corrosion Science*, Vol. 76, pp. 267-274.

Ballim, Y. (1993), "Curing and the durability of OPC, fly ash and blast-furnace slag concretes", *Materials and Structures*, Vol. 26 No. 158, pp. 238-244.

BS EN 1504-5 (2013), "Products and systems for the protection and repair of concrete structures, definitions, requirements, quality control and conformity, Concrete Injection (British Standard).

Cairns, J., Plizzari, G.A., Du, Y., Law, D.W. and Frnazoni, C. (2005), "Mechanical properties of corrosion-damaged reinforcement", *ACI Materials Journal*, Vol. 102 No. 4, pp. 256-264.

Cobo, A., Moreno, E. and Canovas, M. (2011), "Mechanical properties variation of B500SD high ductility reinforcement regarding its corrosion degree", *Materiales de Construcion*, Vol. 61 No. 304, pp. 517-532.

DuraCrete (2000), "The European Union-Brite EuRam III", DuraCrete final technical report, Document BE95-1347/R17.

Du, Y.G., Clark, L.A. and Chan, A.H.C. (2005a), "Effect of corrosion on ductility of reinforcing bars", *Magazine of Concrete Research*, Vol. 57 No. 7, pp. 407-419.

Du, Y.G., Clark, L.A. and Chan, A.H.C. (2005b), "Residual capacity of corroded reinforcing bars", *Magazine of Concrete Research*, Vol. 57 No. 3, pp. 135-147.

El-Sakhawy, N.R., El-Dien, H.S., Ahmed, M.E. and Bendary, K.A. (1999), "Influence of curing on durability performance of concrete", *Magazine of Concrete Research*, Vol. 51 No. 5, pp. 309-318.

Francois, R. and Arliguie, G. (1999), "Effect of microcracking and cracking on the development of corrosion in reinforced concrete members", *Magazine of Concrete Research*, Vol. 51 No. 2, pp. 143-150.

Ghods, P., Isgor, O.B., Mcrae, G.A. and Cu, G.P. (2010), "Electrochemical investigation of chloride-induced depassivation of black steel rebar under simulated service conditions", *Corrosion Science*, Vol. 52 No. 5, pp. 1649-1659.

ISO/FDIS 15630-1 (2002), "International standard. Steel for the reinforcement and prestressing of concrete – test methods. Part 1: reinforcing bars, wire rod and wire".

Kolotyrkin, Y.M. and Popov, Y.A. (1982), "Current development in electrochemistry and corrosion", in Kolotyrkin, Y.M. (Ed.), *Advances in Physical Chemistry*, MIR Publisher, Moscow, p. 11.

Kwon, S.J., Na, U.J., Park, S.S. and Jun, S.H. (2009), "Service life prediction of concrete wharves with early-aged crack: probabilistic approach for chloride diffusion", *Structural Safety*, Vol. 31 No. 1, pp. 75-83.

Law, D.W., Cairns, J., Millard, S.G. and Bungey, J.H. (2004), "Measurement of loss of steel from reinforcing bars in concrete using linear polarisation resistance measurements", *NDT & E International*, Vol. 37 No. 5, pp. 381-388.

Lee, H.S. and Cho, Y.S. (2009), "Evaluation of the mechanical properties of steel reinforcement embedded in concrete specimen as a function of the degree of reinforcement corrosion", *International Journal of Fracture*, Vol. 157 No. 1, pp. 81-88.

Moreno, M., Morris, W., Alvarez, M.G. and Duffo, G.S. (2004), "Corrosion of reinforcing steel in simulated concrete pore solutions: effect of carbonation and chloride content", *Corrosion Science*, Vol. 46 No. 11, pp. 2681-2699.

MTO, SSP 904S13 (1995), "High performance concrete, amendment to OPSS904 construction specification for concrete structures", Ontario Provincial Standard Specification.

Ormellese, M., Berra, M., Bolzoni, F. and Pastore, T. (2006), "Corrosion inhibitors for chlorides induced corrosion in reinforced concrete structures", *Cement and Concrete Research*, Vol. 36 No. 3, pp. 536-547.

Ozbolt, J., Balabanic, G., Periskic, G. and Kuster, M. (2010), "Modelling the effect of damage on transport processes in concrete", *Journal Construction and Building Materials*, Vol. 24 No. 9, pp. 1638-1648.

Papadakis, V.G. (2000), " Effect of supplementary cementing materials on concrete resistance against carbonation and chloride ingress", *Cement and Concrete Research*, Vol. 30 No. 2, pp. 291-298.

Papadopoulos, M.P., Apostolopoulos, C.A., Zervaki, A.D. and Haidemenopoulos, G.N. (2011), "Corrosion of exposed rebars, associated mechanical degradation and correlation with accelerated corrosion tests", *Journal Construction and Building Materials*, Vol. 25 No. 8, pp. 3367-3374.

Poursaee, A. and Hansson, C.M. (2008), "The influence of longitudinal cracks on the corrosion protection afforded reinforcing steel in high performance concrete", *Cement and Concrete Research*, Vol. 38 Nos 8/9, pp. 1098-1105.

Ramezanianpour, A.A. and Malhotra, V.M. (1995), "Effect of curing on the compressive strength resistance to chloride – ion penetration and porosity of concretes incorporating slag, fly ash or silica fume", *Cement & Concrete Composites*, Vol. 17 No. 2, pp. 125-133.

RILEM (2003), "RILEM TC 154-EMC", *Material Structures*, Vol. 36, p. 461.

RILEM (2004), "RILEM TC 154-EMC", *Material Structures*, Vol. 37, p. 623.

Rostam, S. (2003), "Reinforced concrete structures – shall concrete remain the dominating means of corrosion prevention", *Materials and Corrosion*, Vol. 54 No. 6, pp. 369-378.

Rusteel Project (2009-2012), "Effects of corrosion on low-cycle fatigue (seismic) behaviour of high strength steel reinforcing bars", RFS-PR-8017.

Ryell, J., Thomas, M.D.A. and Trunk, P.R. (1999), "Properties of and Service Life Predictions for High Performance Concrete in Transportation Structures", *8th International Conference on Durability of Building Materials and Composites, NRC Research Press*, *Vancouver*.

Schmutz, P. (2013), "Surfaces, interfaces, and their applications II pitting corrosion", Laboratory for Joining Technologies and Corrosion, EMPA Dübendorf.

Shi, X., Xie, N., Fortune, K. and Gong, J. (2012), "Durability of steel reinforced concrete in chloride environments: an overview", *Journal Construction and Building Materials*, Vol. 30, pp. 125-138.

Silva, N. (2013), "Chloride induced corrosion of reinforcement steel in concrete", thesis for degree of doctoral of philosophy, Department of Civil and Environment Engineering, Chalmers University of Technology, Gothenburg.

Stewart, M.G. and Al-Harthy, A. (2008), "Pitting corrosion and structural reliability of corroding RC structures: experimental data and probabilistic analysis", *Reliability Engineering & System Safety*, Vol. 93 No. 3, pp. 373-382.

Strehblow, H.H. (1995), in Marcus, P. and Oudar, J. (Eds), *Corrosion Mechanisms in Theory and Practice*, Marcel Dekker, New York, NY, p. 201.

Turnbull, A., McCartney, L.N. and Zhou, S. (2006), "Modelling of the evolution of stress corrosion cracks from corrosion pits", *Scripta Materialia*, Vol. 54 No. 4, pp. 575-578.

Valcarce, M.B. and Vazquez, M. (2009), "Carbon steel passivity examined in solutions with a low degree of carbonation: the effect of chloride and nitrite ions", *Materials Chemistry and Physics*, Vol. 115 No. 1, pp. 313-321.

Webb, E.G., Paik, C.H. and Alkire, R.C. (2001), "Local detection of dissolved sulfur species from inclusions in stainless steel using Ag microelectrode", *Electrochemical Solid-State Letters*, Vol. 4 No. 4, pp. B15-B18.

Win, P.P., Watanabe, M. and Machida, A. (2004), "Penetration profile of chloride ion in cracked reinforced concrete", *Cement and Concrete Research*, Vol. 34 No. 7, pp. 1073-1079.

Wranglen, G. (1969), "Review article on influence of sulphide inclusions on corrodibility of Fe and steel", *Corrosion Science*, Vol. 9 No. 8, pp. 585-592.

Wranglen, G. (1974), "Pitting and sulfide inclusions in steel", *Corrosion Science*, Vol. 14 No. 5, pp. 331-349.

Xu, J., Jiang, L., Wang, W. and Jiang, Y. (2011), "Influence of $CaCl_2$ and NaCl from different sources on chloride threshold value for the corrosion of steel reinforcement in concrete", *Journal Construction and Building Materials*, Vol. 25 No. 2, pp. 663-669.

Further reading

CEN EN 197-1 (2000), "European standard for cement – Part 1: composition, specifications and conformity criteria for common cements", Europ.Com. Standard, Brusells.

Corresponding author

Alkiviadis Apostolopoulos can be contacted at: prothesis.apostolopoulos@gmail.com